

# The CCL2-CCR2 axis contributes to acquired osimertinib resistance in lung cancer by upregulating Zeb1 expression

**Tzu-Hua Chang**

National Taiwan University Hospital

**Meng-Feng Tsai**

Da-Yeh University

**Shang-Gin Wu**

National Taiwan University Hospital

**Yi-Nan Liu**

National Taiwan University Hospital

**Huey-Dong Wu**

National Taiwan University Hospital

**Tzu-Hsiu Tsai**

National Taiwan University Hospital

**Pei-Hua Lu**

National Taiwan University Hospital

**Han-Nian Jheng**

National Taiwan University Hospital

**Chia-Lang Hsu**

National Taiwan University Hospital, National Taiwan University

**Pu Sheng Yeh**

Min-Sheng General Hospital

**Jin-Yuan Shih** (✉ [jyshih@ntu.edu.tw](mailto: jyshih@ntu.edu.tw))

National Taiwan University Hospital

---

## Research Article

**Keywords:** STAT3, epidermal growth factor receptor, Tyrosine kinase inhibitor, cytokine signalling pathways

**Posted Date:** December 1st, 2023

**DOI:** <https://doi.org/10.21203/rs.3.rs-3674324/v1>

**License:** © ⓘ This work is licensed under a Creative Commons Attribution 4.0 International License.

[Read Full License](#)

**Additional Declarations:** No competing interests reported.

---

**The CCL2-CCR2 axis contributes to acquired osimertinib resistance in lung cancer by  
upregulating Zeb1 expression**

Tzu-Hua Chang<sup>1</sup>, Meng-Feng Tsai<sup>2</sup>, Shang-Gin Wu<sup>1,3</sup>, Yi-Nan Liu<sup>1</sup>, Huey-Dong Wu<sup>5</sup>, Tzu-Hsiu Tsai<sup>1</sup>,  
Pei-Hua Lu<sup>1</sup>, Han-Nian Jheng<sup>1</sup>, Chia-Lang Hsu<sup>6</sup>, Pu Sheng Yeh<sup>7</sup> and Jin-Yuan Shih<sup>1,4,\*</sup>

5

**Affiliation of authors:**

<sup>1</sup> Department of Internal Medicine, National Taiwan University Hospital, Taipei, Taiwan

<sup>2</sup> Department of Biomedical Sciences, Da-Yeh University, Changhua, Taiwan

<sup>3</sup> Department of Internal Medicine, National Taiwan University Cancer Center, Taipei, Taiwan

10 <sup>4</sup> Graduate Institute of Clinical Medicine, College of Medicine, National Taiwan University, Taipei,  
Taiwan

<sup>5</sup> Department of Integrated Diagnostics & Therapeutics, National Taiwan University Hospital, Taipei,  
Taiwan

15 <sup>6</sup> Department of Medical Research, National Taiwan University Hospital, National Taiwan University,  
Taipei, Taiwan

<sup>7</sup> Department of Critical Care Medicine, Min-Sheng General Hospital, Taoyuan, Taiwan.

**\* Corresponding Author:**

20 Jin-Yuan Shih, M.D. Ph.D.,

Department of Internal Medicine, National Taiwan University Hospital, College of Medicine, National

Taiwan University, No. 7, Chung-Shan South Road, Taipei 10002, Taiwan

Tel: +886-2-23562905

Fax: +886-2-23582867

E-mail: jyshih@ntu.edu.tw

5

**Abbreviations:** NSCLC, non-small-cell lung cancer; EGFR, epidermal growth factor receptor; TKI, tyrosine kinase inhibitor; FBS, fetal bovine serum; PVDF, polyvinylidene fluoride; PARPs, poly-ADP-ribose polymerases; EGF, epidermal growth factor; MPEs, malignant pleural effusions; ATCC, American Type Culture Collection.

10

## Abstract

Osimertinib, a third-generation epidermal growth factor receptor (EGFR) tyrosine kinase inhibitor (TKI), effectively treats non-small-cell lung cancer patients with EGFR activation mutations or those with acquired T790M resistance mutation following EGFR-TKIs therapy. However, the development of drug resistance remains a significant clinical challenge. Therefore, we aimed to investigate novel cytokine signaling pathways contributing to osimertinib resistance in lung cancer. Our findings revealed that the CCL2-CCR2 signaling pathway is pivotal in osimertinib resistance development. We observed elevated CCL2 expression in EGFR TKIs-resistant lung cancer cells compared to treatment-naive EGFR mutant cells. Furthermore, ectopic expression of CCL2 in osimertinib-sensitive lung cancer cells conferred resistance to osimertinib in vitro and in vivo. CCL2 knockdown improved osimertinib-induced apoptosis in lung cancer cells. Osimertinib-resistant cells exhibited epithelial-mesenchymal transition phenotypes. We demonstrated that CCL2 primarily confers osimertinib resistance through CCR2, STAT3, and ERK, upregulating Zeb1 expression. Finally, combining a STAT3 inhibitor with osimertinib overcoming resistance in vivo. In conclusion, CCL2 significantly contributes to acquired osimertinib resistance in lung cancer. Targeting the CCL2-CCR2-STAT3/ERK-Zeb1 signaling pathway holds therapeutic potential for overcoming osimertinib resistance and improving treatment outcomes.

**Keywords:** STAT3; epidermal growth factor receptor; Tyrosine kinase inhibitor; cytokine signalling pathways

## 1. Introduction

Lung cancer remains the leading cause of cancer-related deaths worldwide, with a dismal five-year survival rate of only 10–20% in most countries. Non-small-cell lung cancer (NSCLC) constitutes approximately 85% of all lung cancer cases [1, 2]. Unfortunately, traditional treatment options such as surgery, radiation therapy, and platinum-based chemotherapy have limited effectiveness and yield poor prognoses [3]. Given these challenges, molecular-targeted therapies have emerged as a promising approach for patients with NSCLC. The epidermal growth factor receptor (EGFR) is a well-established molecular target in NSCLC owing to its association with cancer development and progression [4]. EGFR somatic activating mutations are prevalent in 40–50% of patients with non-squamous NSCLC in Asia and 10–20% in Western countries [5, 6]. These patients have exhibited favorable responses to EGFR-tyrosine kinase inhibitors [7]. However, a significant drawback is that most patients with NSCLC treated with first- or second-generation EGFR-tyrosine kinase inhibitors (TKIs) eventually develop acquired resistance, with approximately 50–60% acquiring T790M mutation [8]. Osimertinib, a third-generation EGFR-TKI, has demonstrated effectiveness in treating NSCLC patients with T790M mutation [9] and treatment-naïve EGFR mutations [10]. Nonetheless, despite the initial positive response, patients inevitably develop acquired resistance to osimertinib. The mechanisms underlying this resistance can be diverse and complex, involving both EGFR-dependent pathways [8, 11] and EGFR-independent mechanisms [12, 13]. Other contributing factors include alterations in other tyrosine kinase receptors [14, 15], oncogenic fusions [16, 17], and induction of epithelial-mesenchymal transition (EMT) [18]. Additionally, nearly 50% of patients with NSCLC develop osimertinib resistance for reasons that are currently unknown, highlighting the

importance of further investigation to uncover novel mechanisms of acquired resistance to osimertinib.

Chemokine C-C motif ligand 2 (CCL2), also known as monocyte chemoattractant protein-1 (MCP1), belongs to the CC chemokine family [19]. This chemokine plays a significant role in immune cell recruitment, inflammation, and tumor progression [20]. Recent investigations have elucidated that CCL2 is involved in mediating drug resistance in various cancer types [21]. CCL2 can modulate the tumor microenvironment by facilitating the recruitment of immunosuppressive cells, such as tumor-associated macrophages, which contribute to drug resistance through paracrine signaling [22, 23]. Additionally, elevated CCL2 expression has been associated with reduced sensitivity to chemotherapeutic drugs [24-26]. The effects of CCL2 on chemotherapeutic drugs have been studied; however, its impact on EGFR TKIs, particularly osimertinib, has not been adequately explored. Further investigation is necessary to enhance our understanding of the role of CCL2 in osimertinib resistance and the underlying mechanisms involved.

EMT is a complex cellular process that facilitates the conversion of epithelial cells into mesenchymal cells and plays a fundamental role in various biological processes, including embryonic development, tissue repair, and cancer metastasis [27]. Notably, emerging evidence suggests a strong association between CCL2 and EMT induction and regulation [22, 28]. CCL2 directly stimulates EMT by activating ERK-GSK3 $\beta$ -Snail signaling pathways in human breast carcinoma cells [29]. Through binding to its receptor, CCR2, CCL2 initiates downstream events that promote the loss of epithelial markers and the acquisition of mesenchymal characteristics [30].

This study aimed to elucidate the novel CCL2-CCR2 signaling pathway associated with osimertinib resistance in lung cancer. Additionally, we focused on understanding the mechanism by which CCL2, in conjunction with its receptor CCR2, activates downstream signaling pathways. Understanding the specific role of the CCL2-CCR2 pathway in osimertinib resistance is pivotal for devising strategies to overcome or circumvent this resistance mechanism.

## 2. Material and Methods

### 2.1 Chemicals and Cell lines

Osimertinib, INCB3344 (CCR2 antagonist), and S3I-201 (STAT3 inhibitor) were purchased from Selleck Chemicals (Houston, Texas). Recombinant human CCL2 protein was purchased from Peprotech (Rocky Hill, NJ). Human lung cancer cell lines H1975 harboring *EGFR* L858R and T790M mutations and HCC827 harboring *EGFR* exon 19 mutation were purchased from the ATCC (Manassas, VA). The gefitinib-resistant HCC827/gef cells were selected from their parental HCC827 cells after exposure to stepwise escalating concentrations of gefitinib up to 10  $\mu$ M. HCC827/gef cells were cross-resistant to osimertinib [31]. The osimertinib-resistant H1975/AZD cells were developed from the parental cells subjected to persistent gradient exposure to osimertinib for about 6 months by increasing osimertinib concentration up to 3  $\mu$ M [15]. Single clones of osimertinib-resistant H1975/AZD-15 and H1975/AZD-18 cells were obtained by isolating single cells from H1975/AZD mixed clones using a serial dilution method.

HCC827-CCL2 cells were generated by transfecting them with a plasmid carrying human CCL2



cDNA (SC118317, Origene, Rockville, MD). After transfection, these cells were selected over 14 days using geneticin-containing media. Subsequently, the cells were cultured in RPMI 1640 medium supplemented with 5% fetal bovine serum (FBS), 100 U/mL penicillin, and 100 µg/mL streptomycin (Gibco, Grand Island, NY). The cell cultures were maintained at 37°C in a humidified incubator with 5% CO<sub>2</sub>.

## ***2.2 Small interfering RNA (siRNA) and transfection***

Small interfering RNA (siRNA) specific for CCL2 (ID: s12565, ID:s12566) or Zeb1 (ID:s229971) was purchased from Life Technology. CCR2 siRNA was provided by Dharmacon (Chicago, IL). The siRNA was transfected into cells using Lipofectamine RNAiMAX Reagent (Life Technologies, CA) according to the manufacturer's instructions.

## ***2.3 Cytotoxicity assays***

The cells were first plated at a density of 3000–5000 cells per well in 96-well plates. Subsequently, the cells were treated with various concentrations of drugs. After 48–72 h of treatment, cell viability was determined using 3-(4,5-Dimethylthiazol-2-yl)-2,5-diphenyltetrazolium bromide (MTT) assays (Merck Millipore, Darmstadt, Germany) according to the manufacturer's instructions. Finally, the absorbance was measured at 570 nm using a SpectraMax i3x Multi-Mode Microplate Reader (Molecular Device, CA). The cell survival percentages are represented as mean±SD (SD, standard deviation).

## ***2.4 Western blotting***

Cells were lysed in RIPA buffer (Cell Signaling Technology, Danvers, MA) with 1% phosphatase inhibitor cocktail. Lysates containing 20–30 µg protein were loaded onto 6–12% sodium dodecyl sulfate-polyacrylamide gels electrophoresis, and the separated proteins were then transferred to polyvinylidene fluoride (PVDF) membranes (Pall, NY). After blocking with 5% fat-free milk for 1 h, the membranes were incubated with the primary antibody overnight at 4°C and then with the peroxidase-labeled secondary antibody 1h at room temperature (Agilent, CA). All antibodies used in the study are listed in Table S1. Western blotting bands were visualized using ECL select western blotting detection reagent (Merck).

## ***2.5 ELISA***

We used 24-hour cell-conditioned media that were controlled for cell number and media volume to detect CCL2 using human CCL2 enzyme-linked immunosorbent assay (ELISA) kits (R&D Systems) according to the manufacturer's instructions. Absorbance was read at an optical density of 450 nm using a SpectraMax i3x Multi-Mode Microplate Reader. The concentration of each conditioned media was determined by referring to a standard curve and is represented as the mean ± SD.

## ***2.6 Cell apoptosis assay***

HCC872/gef cells were transfected with CCL2 siRNA for 48 h and then exposed to 250 nM osimertinib for another 24 h. The Annexin V-FITC apoptosis detection Kit (BD Bioscience) was used to detect apoptosis, following the manufacturer's protocol. Subsequently, the cells were analyzed using an Attune™ NxT Flow Cytometer (Life Technologies).

5

### ***2.7 Caspase-Glo 9 Assay***

The caspase-9 activity in cell lysates was assayed using the Caspase 9-Glo luminescent kit (Promega, Madison, WI), following the manufacturer's instructions. Cells were seeded in 96-well plates and subsequently treated with osimertinib for 18 h. After incubation, the cells were lysed. Luminescence values were measured using the SpectraMax i3x Multi-Mode Microplate Reader equipped for luminescence detection.

10

### ***2.8 RNA isolation and Quantitative real-time PCR***

Total RNA was extracted using Trizol reagent (Life Technologies) according to the manufacturer's instructions. The reverse transcription reaction was performed using 1 µg of total RNA with a Quantscript RT kit (Qiagen Biotechnology, Dusseldorf, Germany). The mRNA expression level was determined by quantitative real-time PCR using SYBR Green Master Mix (Applied Biosystems, CA) and a Quantstudio 7 flex real-time PCR system (Applied Biosystems). The sequences of the gene-specific primers used in the study are listed in Table S2.

15

## ***2.9 Xenograft animal studies***

All animal procedures were approved by the Institutional Animal Care and Use Committee (IACUC) of the National Taiwan University College of Medicine, Taiwan, and performed in compliance with the IACUC guidelines. Cancer cells (HCC827-mock, HCC827-CCL2, and H9175/AZD-18) were injected subcutaneously into the lower rear flank of 5-week-old severe combined immune deficient (SCID) athymic male mice from BioLASCO (Taiwan). The animals were randomized into groups 14–21 days after tumor-cell injection when tumors had grown to approximately 200 mm<sup>3</sup>. Tumor volumes were evaluated after treatment with osimertinib or S3I-201. Tumor volume and mouse weight were recorded every 4 days, and tumor volumes were assessed using the formula  $\text{mm}^3 = \text{width}^2 \times \text{length} / 2$ .

## ***2.10 Malignant pleural effusion isolation***

We consecutively collected pleural effusion using thoracentesis in the chest ultrasonography examination room at the National Taiwan University Hospital. Before thoracentesis, all enrolled patients signed informed consent forms for future molecular analysis, which was approved by the Institutional Review Board of the National Taiwan University Hospital. The cytology of pleural effusion showing adenocarcinoma of the lung was used in this study.

First, we used RBC lysis buffer for hemolysis of red blood cells in the pleural effusions. Next, the remaining cells were washed twice using PBS and cultured in complete RPMI1640 media [32]. The

medium was replaced every 2–3 days, and the cells were harvested after 10 days. Subsequently, we used Trizol reagent (Invitrogen, NY) to extract total RNA from cultured cells. Reverse transcription-quantitative polymerase chain reaction (RT-qPCR) was used to analyze the expression of CCL2 using TaqMan CCL2 probes (Life Technologies) on an Applied Biosystems QuantStudio 7 Flex.

## 5 **2.12 Statistical analysis**

Data are presented as the mean  $\pm$  SD for *in vitro* and *in vivo* experiments. The statistical comparison between the two groups was assessed using the unpaired Student's t-test. Clinical data were presented as the group's median, and the statistical comparison between the two groups was performed using the Mann–Whitney U test. Statistical significance was set at  $p < 0.05$ . All statistical analyses were conducted using SPSS software (version 22.0, SPSS Inc., Chicago, IL).

## **3. Results**

### **3.1 CCL2 expression is significantly increased in osimertinib-resistant cells**

In previous studies, we established osimertinib-resistant cell lines, including HCC827/gef and clones (H1975/AZD-15 and H1975/AZD-18) [15, 33]. These cell lines exhibited vigorous growth in the presence of osimertinib, confirming their drug-resistance characteristics. The sensitive parental cells H1975 and HCC827 were significantly susceptible to osimertinib at concentrations below 30 nM. However, the EGFR TKI-resistant cells (HCC827/gef, H1975/AZD-15, and H1975/AZD-18) demonstrated resistance to osimertinib, with  $IC_{50}$  values greater than 1  $\mu$ M (Fig. 1A and 1E). To identify EGFR TKI resistance-

associated genes, we analyzed four expression datasets (GSE80344, GSE106765, GSE103350, and GSE95558). Gene scores were calculated based on expression levels, and a discounted rating system was used to combine rankings [34]. Among the top 100 upregulated genes, a set of genes were involved in tumor microenvironment and immune cytokine pathway, including S100A8, IL1A, IL1B, and CCL2 (Table S3). Here, we verified that CCL2 is upregulated in osimertinib-resistant cells. The expression levels of CCL2 mRNA and protein were found to be upregulated in HCC827/gef cells (Fig. 1B, 1D), as well as in H1975/AZD-15 and H1975/AZD-18 (Fig. 1F, 1H), compared to the parental HCC827 and H1975 cells, respectively. Additionally, CCL2 secretion was significantly increased in HCC827/gef (Fig. 1C) and H1975/AZD-15, H1975/AZD-18 cells (Fig. 1G) compared to parental HCC827 and H1975 cells, as determined by ELISA assay. These findings provide evidence that CCL2 expression is elevated in acquired resistance to osimertinib *in vitro*.

### ***3.2 CCL2 upregulation in malignant pleural effusion of lung adenocarcinoma following resistance to osimertinib and 1st/2nd-generation EGFR TKIs***

We collected 63 malignant pleural effusions (MPEs) from patients with lung adenocarcinoma harboring EGFR mutations. Of these, 26 MPEs were obtained at the initial diagnosis of lung cancer before systemic treatment, 16 were collected after the patient acquired resistance to osimertinib, and 21 were obtained from those who showed resistance to first- or second-generation EGFR-TKIs (erlotinib: 10, gefitinib: 10, and afatinib: 1). There were no significant differences in the clinical characteristics of the

patients between the three groups (Table S4). The CCL2 expression levels of the primary cancer cells isolated from MPEs were detected using RT-qPCR. The results indicated that the median CCL2 expression level was significantly higher in MPEs collected from patients who had acquired resistance to osimertinib than in those obtained from treatment-naïve pleural effusions ( $p = 0.0142$ , by Mann–Whitney U test, Fig. 1I). Additionally, the results demonstrated that MPEs collected from patients after acquiring resistance to first- or second-generation EGFR-TKIs had significantly higher median expression of CCL2 ( $p = 0.0090$ , by Mann–Whitney U test, Fig. 1I).

### 3.3. *Elevated expression of CCL2 contributes to the acquisition of osimertinib resistance in osimertinib-sensitive cells*

To validate the significance of CCL2 in osimertinib resistance, we conducted experiments involving CCL2-overexpressing transfectants (HCC827-CCL2) and control transfectants (HCC827-mock; Fig. 2A). By introducing CCL2 in osimertinib-sensitive HCC827 cells, we observed that these cells exhibited resistance to osimertinib, as determined by MTT assay (Fig. 2B). Furthermore, to validate these findings, we investigated the effect of CCL2 on osimertinib-induced apoptosis in osimertinib-sensitive cells (HCC827). Our results demonstrated that CCL2 significantly attenuated caspase 9 activity induced by osimertinib in these cells (Fig. 2C). We conducted *in vivo* experiments to further confirm the role of CCL2 in promoting cell proliferation in the absence (Fig. 2D) or presence of osimertinib (Fig. 2E). There was no significant difference in tumor growth curves between mice injected with HCC827-mock cells and

those injected with CCL2-overexpressing HCC827 cells (Fig. 2D). Notably, osimertinib administration effectively suppressed tumor growth and reduced tumor weight in mice injected with HCC827-mock cells but had limited impact on those injected with CCL2-overexpressing HCC827 cells (Fig. 2E and 2F). These results collectively demonstrate that the elevated expression of CCL2 attenuated the inhibitory effects of osimertinib in lung cancer cells.

### ***3.4. CCL2 knockdown in osimertinib-resistant cells enhanced osimertinib responsiveness***

As shown in Fig. 3A, 3F and 3I, the transient transfection of CCL2 siRNA into osimertinib-resistant cells (HCC827/gef, H1975/AZD-15, and H1975/AZD-18) resulted in lower levels of CCL2 expression compared to the control cells (HCC827/gef-si-scramble, H1975/AZD-15-si-scramble and H1975/AZD-18-si-scramble). Notably, the knockdown of CCL2 in osimertinib-resistant cells led to increased cell death upon treatment with osimertinib (Fig. 3B, 3G, and 3J). In HCC827/gef cells, the downregulation of CCL2 expression promoted osimertinib-induced apoptosis as evidenced by luminescent and caspase-glo 9 assay and Annexin V-FITC apoptosis assay (Fig. 3C, 3D). Additionally, osimertinib-induced cleavages of PARP and caspase-3 were significantly increased in HCC827/gef, H1975/AZD-15, and H1975/AZD-18 cells after CCL2 knockdown by transfection of CCL2 siRNA (Figure 3E, H, and K). These results highlight the functional importance of CCL2 in maintaining osimertinib resistance in osimertinib-resistant cells. Targeting CCL2 could potentially be a therapeutic approach to overcome osimertinib resistance in lung cancer.



### **3.5. CCL2 confers osimertinib resistance through Zeb1 upregulation**

As shown in Fig. 4A and 4B, osimertinib-resistant cells (H1975/AZD-15, H1975/AZD-18, and HCC827/gef) displayed distinct morphological changes compared to osimertinib-sensitive cells. These resistant cells exhibited a loss of cell-cell contacts and acquired an elongated, spindle-shaped mesenchymal phenotype, characteristic of cells undergoing EMT. Previous studies have provided evidence linking the EMT process to both primary and acquired resistance to EGFR TKIs [33, 35-37]. The transition to the mesenchymal phenotype in osimertinib-resistant cells was accompanied by decreased expression of the epithelial marker E-cadherin and increased expression of the mesenchymal markers Vimentin and Zeb1 (Fig.4A and 4B). These markers are well-established indicators of the EMT process.

CCL2 has been implicated in the EMT process in various cancer cell types, including head and neck squamous cell carcinomas [38], breast carcinoma cells [29], and glioblastoma [39]. We investigated the effect of CCL2 stimulation on EMT progression in drug-sensitive cancer cells. CCL2-overexpressing transfectants exhibited higher levels of Zeb1 protein expression (Fig. 4C), whereas CCL2-knockdown transfectants showed lower levels of Zeb1 protein expression (Fig. 4D).

To further investigate the role of Zeb1 in CCL2-mediated osimertinib resistance in drug-sensitive cells, we examined the impact of Zeb1 knockdown on osimertinib-resistant cells. The knockdown of Zeb1 expression in CCL2-overexpressing transfectants (HCC827-CCL2-si-Zeb1) significantly suppressed the CCL2-mediated osimertinib resistance (Fig. 4E and 4F). Furthermore, Zeb1 knockdown increased the

sensitivity of H1975/AZD-18 cells to osimertinib, as evidenced by a significant decrease in the IC<sub>50</sub> values (Fig. 4G and 4H). These results provide evidence that CCL2 mediates osimertinib resistance in lung cancer cells through the up-regulation of Zeb1 expression.

### 5 **3.6. *STAT3 and ERK Signaling Pathway are involved in CCL2 mediates osimertinib resistance***

We further examined the effects of osimertinib on EGFR downstream signaling pathway in both osimertinib-sensitive (H1975 and HCC827) and -resistant cell lines (H1975/AZD-18 and HCC827/gef). Osimertinib treatment inhibited EGFR downstream targets, including phosphorylated EGFR, AKT, ERK, and STAT3 in osimertinib-sensitive cells (H1975 and HCC827), but maintained phosphorylated STAT3  
10 and ERK in osimertinib-resistant cell lines (H1975/AZD-18 and HCC827/gef) (Fig. 5A and 5B). These results suggest that the activation of STAT3 and ERK contributes to osimertinib resistance in these cell lines. Given that CCL2 is known to activate JAK-STAT, MAPK, and PI3K-AKT pathways, which regulate various biological processes [29, 40], we explored whether CCL2 renders EGFR-mutated NSCLC cells resistant to osimertinib by activating EGFR downstream signaling pathways. The results showed that  
15 stimulation with recombinant CCL2 protein led to a clear increase in STAT3 and ERK phosphorylation (Fig. 5C). Similarly, CCL2-overexpressing transfectants expressed higher phosphorylated STAT3 and ERK (Fig. 5D), whereas CCL2-knockdown transfectants expressed lower phosphorylated STAT3 and ERK (Fig. 5E). These results suggest that the activation of the STAT3 and ERK signaling pathways may be associated with CCL2-induced resistance to osimertinib.

### ***3.7. Targeting the CCL2-CCR2 signaling pathway enhances osimertinib-induced cell death and reverses EMT***

To elucidate the role of the CCL2-CCR2 axis in regulating osimertinib resistance, we investigated  
5 by employing CCR2 knockdown using CCR2 siRNA. Our results demonstrated that CCR2 knockdown  
led to a decrease in CCR2 expression, STAT3 phosphorylation, and ERK1/2 phosphorylation (Fig. 6A).  
Additionally, CCR2 knockdown significantly enhanced osimertinib-induced cytotoxicity and caspase-9  
activity in CCL2-overexpressing HCC827 cells (HCC827-CCL2-si-CCR2-1; Fig. 6B, 6C). After  
treatment with the CCR2 antagonist (INCB3344) in HCC827-CCL2 cells, the expression of CCR2  
10 downstream kinases, including p-STAT3, p-ERK1/2, and Zeb1 decreased as shown by western blot (Fig  
4D). To evaluate the efficacy of the combination of INCB3344 with osimertinib in inhibiting cell viability  
in osimertinib-resistant HCC827-CCL2 cells, we treated the cells with both INCB3344 (CCR2 antagonist)  
and osimertinib. The cotreatment with INCB3344 and osimertinib markedly restrained cell survival and  
decreased caspase-9 activity (Fig.6E, 6F). Additionally, the STAT3 inhibitor (S3I-201) effectively  
15 suppressed CCL2-induced Zeb1 expression (Fig. 6G) and reversed CCL2-mediated resistance to  
osimertinib (Fig. 6H). To further investigate the ability of the STAT3 inhibitor to restore the sensitivity  
of osimertinib-resistant cells to osimertinib *in vivo*, xenograft tumors were generated by injecting  
H1975/AZD-18 cells into SCID mice. Consistent with the *in vitro* findings, treatment with osimertinib  
alone did not effectively inhibit the growth of H1975/AZD-18 tumors. However, when the mice were

treated with a combination of STAT3 inhibitor S3I-201 and osimertinib, significant inhibition of tumor growth was observed (Fig. 6I). These results provide compelling evidence that the combination of the STAT3 inhibitor and osimertinib is capable of suppressing the growth of osimertinib-resistant NSCLC xenografts in an *in vivo* model. Selumetinib (ERK inhibitor) effectively suppressed CCL2-induced Zeb1 expression in HCC827-CCL2 cells (Fig. 6J) and reversed CCL2-mediated resistance to osimertinib (Fig. 6K). These findings indicate that the CCL2/CCR2 axis results in resistance to osimertinib in drug-sensitive cells by activating the STAT3 and ERK pathways.

To investigate the significance of the CCL2-CCR2 axis in mediating EMT, we performed experiments by employing CCR2 knockdown using CCR2 siRNA. Knocking down CCR2 resulted in the reversal of the EMT phenotype, as demonstrated by an increased expression of the epithelial marker E-cadherin and a decrease in the mesenchymal marker vimentin, in comparison to HCC827-CCL2 cells expressing a control siRNA (Fig. S1A). Furthermore, to elucidate the downstream signaling pathways of CCL2 contributing to the promotion of the EMT process, we performed intervention assays using INCB3344, S3I-201, and selumetinib. The reversal of EMT markers was observed in Fig. S1B–D. These results suggest that the CCL2-CCR2 axis mediates the EMT process through the STAT3 and ERK pathways.

Targeting the CCL2-CCR2 signaling axis significantly enhanced osimertinib-induced cell death and reversed EMT in lung cancer cells. A summary diagram of the CCL2–CCR2-Zeb1 axis and the potential

pathways in osimertinib-resistant cells are shown in Figure 7. The CCL2-CCR2 axis contributes to the acquisition of osimertinib resistance in lung cancer by activating STAT3 and ERK signaling.

#### 4. Discussion

5 In this study, we investigated the role of CCL2 in the development of resistance to osimertinib in lung cancer. Higher levels of CCL2 expression were present in osimertinib-resistant cell lines, and its expression increased following osimertinib resistance development in patients. Moreover, the cells became more sensitive to osimertinib when CCL2 expression was suppressed in osimertinib-resistant cells using genetic silencing techniques. These results suggest that CCL2 played a role in mediating osimertinib  
10 resistance in lung cancer. Additionally, we investigated the molecular mechanisms underlying the effects of CCL2 in osimertinib resistance. Our findings indicated that CCL2 upregulated Zeb1 expression by activating the STAT3 and ERK pathways. Pharmacological inhibition was performed to block CCR2, STAT3, and ERK signaling in CCL2-mediating osimertinib resistance cells, which significantly enhanced the ability of osimertinib to induce cell death. In summary, this study uncovered a novel cytokine pathway  
15 involving CCL2-CCR2-STAT3/ERK-Zeb1 that contributes to osimertinib resistance in lung cancer. Targeting the CCL2-CCR2 signaling axis can potentially enhancing the efficacy of osimertinib treatment and overcoming resistance (Fig. 7).

Increasing evidence demonstrates that CCL2 is an essential component of the tumor microenvironment. The increased expression of CCL2 in the tumor microenvironment significantly  
20 impacts the effectiveness of trastuzumab (a HER2 monoclonal antibody) by promoting the recruitment of

immunosuppressive cells, thereby dampening its anti-tumor effects in HER2-positive gastric cancer [42,43]. Additionally, CCL2 plays a pivotal role in promoting hepatocellular carcinoma progression and sorafenib resistance by enhancing tumor cell survival, migration, and invasion [41, 42]. Moreover, heightened CCL2 levels can counteract the anti-angiogenic effects of bevacizumab (a drug targeting vascular endothelial growth factor) in colorectal cancer [43]. CCL2 plays a significant role in driving resistance to targeted therapies and facilitating tumor progression; however, its role in osimertinib-resistant lung cancer has not been thoroughly evaluated. In this study, we demonstrated that the increased expression of CCL2 contributes to the acquisition of osimertinib resistance in initially osimertinib-sensitive cells. Furthermore, knocking down CCL2 in osimertinib-resistant cells led to an enhancement of osimertinib responsiveness. Our research findings provide valuable insights into the significance of the CCL2-CCR2 signaling pathway in driving the development of resistance to a third-generation EGFR-TKI osimertinib in lung cancer.

Our study also emphasized the connection between CCL2-induced osimertinib resistance and the activation of the STAT3 and ERK signaling pathways. Our results indicated that both the STAT3 and ERK signaling pathways are downstream of CCL2 and are involved in CCL2-mediated osimertinib resistance in lung cancer. Activation of the ERK signaling pathway has been implicated in osimertinib resistance, as evidenced in our study using an osimertinib-resistant cell line model (Fig.6) and supported by the findings of Shi et al. [44] and Huang et al. [45]. These findings suggest that the activation of the CCL2/ERK pathway facilitates the bypassing of EGFR inhibition induced by osimertinib. Additionally, our results

indicated that CCL2 plays a role in the development of osimertinib resistance in lung cancer by activating the STAT3 pathway. Several studies have reported that cancer cells that acquire resistance to EGFR-TKIs (such as gefitinib, erlotinib, afatinib, and osimertinib) often display elevated levels of phosphorylated STAT3. Increased STAT3 activation is frequently associated with acquired resistance to EGFR-TKIs [46-5 49]. Moreover, the findings presented by Sun et al. provide additional evidence supporting this idea, demonstrating that both STAT3 and IL-4 are involved in the development of osimertinib resistance. [50]. In the context of osimertinib resistance, activating the STAT3 signaling pathway confers a survival advantage to tumor cells by inhibiting cell death-associated pathways and orchestrating changes in the tumor microenvironment.

10 Zeb1, a transcription factor linked to the epithelial-mesenchymal transition (EMT), plays a crucial role in enhancing cancer cell invasiveness and confers resistance to targeted therapies [51, 52]. Previous studies have indicated that CD44 promotes lung cancer cell metastasis and may potentially contribute to epithelial-mesenchymal transition (EMT) by activating the ERK-Zeb1 signaling pathway [53]. Following treatment with EGFR inhibitors, the increased expression of Zeb1 leads to alterations in cellular behavior, 15 resulting in reduced reliance on EGFR signaling pathways for survival [52]. Zeb1-mediated EMT has been identified as one of the underlying causes of erlotinib resistance in EGFR-mutant lung cancer cells [51]. Moreover, the activation of the STAT3-Zeb1 signaling pathway enhance EGFR-TKI resistance in lung cancer [58]. Indeed, both the ERK-Zeb1 and STAT3-Zeb1 axes are interconnected and have a significant impact on cancer progression and drug resistance. The alterations in cell behavior induced by EMT

contribute to reduced sensitivity to a variety of targeted therapies. Our findings reveal that CCL2-mediated osimertinib resistance in lung cancer through up-regulating Zeb1 expression. Knockdown of Zeb1 expression in CCL2-overexpressing transfectants significantly suppressed the CCL2-mediated osimertinib resistance. In this study, we also indicated that CCL2 upregulated Zeb1 expression in lung cancer cells through activating STAT3 and ERK signaling pathways. The combination treatment of the STAT3 inhibitor (S3I-201) or ERK inhibitor (selumetinib) with osimertinib in CCL2-mediated osimertinib resistance cells leads to the suppression of CCL2-induced Zeb1 expression and the subsequent reversal of CCL2-mediated resistance to osimertinib.

Our study has demonstrated that the CCL2-CCR2 signaling axis triggers increased phosphorylation of STAT3 and ERK, subsequently leading to enhance Zeb1 expression in lung cancer. It is noteworthy that the CCL2-CCR2 pathway not only contributes to osimertinib resistance but also actively participates in cancer progression. To conclude, our findings strongly support the pivotal role of CCL2 in the development of acquired osimertinib resistance in lung cancer. Targeting the CCL2-CCR2-STAT3/ERK-Zeb1 signaling pathway emerges as a promising therapeutic approach for overcoming osimertinib resistance and enhancing treatment outcomes in this context.

#### **Acknowledgments:**

The authors thank the 2<sup>nd</sup> and 3<sup>rd</sup> Core Facility in the Department of Medical Research, National Taiwan University Hospital, for providing laboratory facilities.



## **Declarations**

### **Ethics approval and informed consent**

The present study adhered to the principles of the Declaration of Helsinki and was approved by the Institutional Review Board (IRB) of the National Taiwan University Hospital. Informed consent was  
5 obtained from all patients who participated in the study before the collection of samples for molecular analysis.

### **Availability of data and materials**

Please contact the corresponding author for data requests.

### **Declaration of Interest Statement**

10 The authors declare no conflict of interest.

### **Funding**

This study was supported by the National Taiwan University Hospital, Taipei, Taiwan (107-S3788, 108-S4257, 108-S4305, 109-S4700), the Collaborative Research Projects of National Taiwan University College of Medicine, National Taiwan University Hospital and Min-Sheng General Hospital. (109F005-  
15 111-P),and the Excellent Translational Medicine Research Projects of the National Taiwan University College of Medicine and National Taiwan University Hospital (112C101-71)

### **Authors' contributions**

TH Chang, and JY Shih designed this study. TH Chang, MF Tsai, YN Liu and JY Shih wrote the paper.

SG Wu, HD Wu, and JY Shih conducted the analysis and interpretation of the clinical data. CL Hsu analyzed the bioinformatics data. All the authors have read and approved the final manuscript. TH Tsai, PH Lu, HN Jheng, and PS Yeh conducted the analysis and interpretation of the in vitro data.

## References

1. Thai AA, Solomon BJ, Sequist LV, Gainor JF, Heist RS: **Lung cancer**. *Lancet* 2021, **398**(10299):535-554.
2. Siegel RL, Miller KD, Wagle NS, Jemal A: **Cancer statistics, 2023**. *CA Cancer J Clin* 2023, **73**(1):17-48.
3. Rossi A, Di Maio M: **Platinum-based chemotherapy in advanced non-small-cell lung cancer: optimal number of treatment cycles**. *Expert Rev Anticancer Ther* 2016, **16**(6):653-660.
4. Cheng WL, Feng PH, Lee KY, Chen KY, Sun WL, Van Hiep N, Luo CS, Wu SM: **The Role of EREG/EGFR Pathway in Tumor Progression**. *Int J Mol Sci* 2021, **22**(23).
5. Rosell R, Moran T, Queralt C, Porta R, Cardenal F, Camps C, Majem M, Lopez-Vivanco G, Isla D, Provencio M *et al*: **Screening for epidermal growth factor receptor mutations in lung cancer**. *N Engl J Med* 2009, **361**(10):958-967.
6. Shi Y, Au JS, Thongprasert S, Srinivasan S, Tsai CM, Khoa MT, Heeroma K, Itoh Y, Cornelio G, Yang PC: **A prospective, molecular epidemiology study of EGFR mutations in Asian patients with advanced non-small-cell lung cancer of adenocarcinoma histology (PIONEER)**. *J Thorac Oncol* 2014, **9**(2):154-162.
7. Mok TS, Wu YL, Thongprasert S, Yang CH, Chu DT, Saijo N, Sunpaweravong P, Han B, Margono B, Ichinose Y *et al*: **Gefitinib or carboplatin-paclitaxel in pulmonary adenocarcinoma**. *N Engl J Med* 2009, **361**(10):947-957.
8. Yu HA, Arcila ME, Rekhtman N, Sima CS, Zakowski MF, Pao W, Kris MG, Miller VA, Ladanyi M, Riely GJ: **Analysis of tumor specimens at the time of acquired resistance to EGFR-TKI therapy in 155 patients with EGFR-mutant lung cancers**. *Clin Cancer Res* 2013, **19**(8):2240-2247.
9. Mok TS, Wu YL, Papadimitrakopoulou VA: **Osimertinib in EGFR T790M-Positive Lung Cancer**. *N Engl J Med* 2017, **376**(20):1993-1994.
10. Ramalingam SS, Vansteenkiste J, Planchard D, Cho BC, Gray JE, Ohe Y, Zhou C, Reungwetwattana T, Cheng Y, Chewaskulyong B *et al*: **Overall Survival with Osimertinib in Untreated, EGFR-Mutated Advanced NSCLC**. *N Engl J Med* 2020, **382**(1):41-50.
11. Wu SG, Liu YN, Tsai MF, Chang YL, Yu CJ, Yang PC, Yang JC, Wen YF, Shih JY: **The mechanism of acquired resistance to irreversible EGFR tyrosine kinase inhibitor-afatinib in lung adenocarcinoma patients**. *Oncotarget* 2016, **7**(11):12404-12413.
12. Leonetti A, Sharma S, Minari R, Perego P, Giovannetti E, Tiseo M: **Resistance mechanisms to osimertinib in EGFR-mutated non-small cell lung cancer**. *Br J Cancer* 2019, **121**(9):725-737.
13. Schmid S, Li JJN, Leighl NB: **Mechanisms of osimertinib resistance and emerging treatment options**. *Lung Cancer* 2020, **147**:123-129.

14. Taniguchi H, Yamada T, Wang R, Tanimura K, Adachi Y, Nishiyama A, Tanimoto A, Takeuchi S, Araujo LH, Boroni M *et al*: **AXL confers intrinsic resistance to osimertinib and advances the emergence of tolerant cells.** *Nat Commun* 2019, **10**(1):259.
15. Liu YN, Tsai MF, Wu SG, Chang TH, Tsai TH, Gow CH, Chang YL, Shih JY: **Acquired resistance to EGFR tyrosine kinase inhibitors is mediated by the reactivation of STC2/JUN/AXL signaling in lung cancer.** *Int J Cancer* 2019, **145**(6):1609-1624.
- 5
16. Liu J, Li X, Peng J: **A Novel CAV1-MET Fusion in SCLC Transformation Responds to Crizotinib and Osimertinib Treatment.** *J Thorac Oncol* 2019, **14**(6):e126-e128.
17. Offin M, Somwar R, Rekhtman N, Benayed R, Chang JC, Plodkowski A, Lui AJW, Eng J, Rosenblum M, Li BT *et al*: **Acquired ALK and RET Gene Fusions as Mechanisms of Resistance to Osimertinib in EGFR-Mutant Lung Cancers.** *JCO Precis Oncol* 2018, **2**.
- 10
18. Jiang XM, Xu YL, Yuan LW, Zhang LL, Huang MY, Ye ZH, Su MX, Chen XP, Zhu H, Ye RD *et al*: **TGF $\beta$ 2-mediated epithelial-mesenchymal transition and NF- $\kappa$ B pathway activation contribute to osimertinib resistance.** *Acta Pharmacol Sin* 2021, **42**(3):451-459.
- 15
19. Hao Q, Vadgama JV, Wang P: **CCL2/CCR2 signaling in cancer pathogenesis.** *Cell Commun Signal* 2020, **18**(1):82.
20. Ozga AJ, Chow MT, Luster AD: **Chemokines and the immune response to cancer.** *Immunity* 2021, **54**(5):859-874.
21. Shi Z, Tu J, Ying Y, Diao Y, Zhang P, Liao S, Xiong Z, Huang S: **CC Chemokine Ligand-2: A Promising Target for Overcoming Anticancer Drug Resistance.** *Cancers (Basel)* 2022, **14**(17).
22. Xu M, Wang Y, Xia R, Wei Y, Wei X: **Role of the CCL2-CCR2 signalling axis in cancer: Mechanisms and therapeutic targeting.** *Cell Prolif* 2021, **54**(10):e13115.
- 25
23. Kadomoto S, Izumi K, Mizokami A: **Roles of CCL2-CCR2 Axis in the Tumor Microenvironment.** *Int J Mol Sci* 2021, **22**(16).
24. Qian Y, Ding P, Xu J, Nie X, Lu B: **CCL2 activates AKT signaling to promote glycolysis and chemoresistance in glioma cells.** *Cell Biol Int* 2022, **46**(5):819-828.
25. Xu W, Wei Q, Han M, Zhou B, Wang H, Zhang J, Wang Q, Sun J, Feng L, Wang S *et al*: **CCL2-SQSTM1 positive feedback loop suppresses autophagy to promote chemoresistance in gastric cancer.** *International Journal of Biological Sciences* 2018, **14**(9):1054-1066.
- 30
26. Moisan F, Francisco EB, Brozovic A, Duran GE, Wang YC, Chaturvedi S, Seetharam S, Snyder LA, Doshi P, Sikic BI: **Enhancement of paclitaxel and carboplatin therapies by CCL2 blockade in ovarian cancers.** *Mol Oncol* 2014, **8**(7):1231-1239.
- 35
27. Ribatti D, Tamma R, Annese T: **Epithelial-Mesenchymal Transition in Cancer: A Historical Overview.** *Transl Oncol* 2020, **13**(6):100773.
28. Tsai YC, Chen WY, Abou-Kheir W, Zeng T, Yin JJ, Bahmad H, Lee YC, Liu YN:

**Androgen deprivation therapy-induced epithelial-mesenchymal transition of prostate cancer through downregulating SPDEF and activating CCL2.** *Biochim Biophys Acta Mol Basis Dis* 2018, **1864**(5 Pt A):1717-1727.

29. Li S, Lu J, Chen Y, Xiong N, Li L, Zhang J, Yang H, Wu C, Zeng H, Liu Y: **MCP-1-**  
5 **induced ERK/GSK-3beta/Snail signaling facilitates the epithelial-mesenchymal transition and promotes the migration of MCF-7 human breast carcinoma cells.** *Cell Mol Immunol* 2017, **14**(7):621-630.
30. Tian X, Wang J, Jiang L, Jiang Y, Xu J, Feng X: **Chemokine/GPCR Signaling-Mediated EMT in Cancer Metastasis.** *J Oncol* 2022, **2022**:2208176.
- 10 31. Liu YN, Tsai MF, Wu SG, Chang TH, Tsai TH, Gow CH, Wang HY, Shih JY: **miR-146b-5p Enhances the Sensitivity of NSCLC to EGFR Tyrosine Kinase Inhibitors by Regulating the IRAK1/NF- $\kappa$ B Pathway.** *Mol Ther Nucleic Acids* 2020, **22**:471-483.
32. Wu SG, Gow CH, Yu CJ, Chang YL, Yang CH, Hsu YC, Shih JY, Lee YC, Yang PC: **Frequent epidermal growth factor receptor gene mutations in malignant pleural**  
15 **effusion of lung adenocarcinoma.** *Eur Respir J* 2008, **32**(4):924-930.
33. Weng CH, Chen LY, Lin YC, Shih JY, Lin YC, Tseng RY, Chiu AC, Yeh YH, Liu C, Lin YT *et al*: **Epithelial-mesenchymal transition (EMT) beyond EGFR mutations per se is a common mechanism for acquired resistance to EGFR TKI.** *Oncogene* 2019, **38**(4):455-468.
- 20 34. Wu SG, Chang TH, Tsai MF, Liu YN, Hsu CL, Chang YL, Yu CJ, Shih JY: **IGFBP7 Drives Resistance to Epidermal Growth Factor Receptor Tyrosine Kinase Inhibition in Lung Cancer.** *Cancers (Basel)* 2019, **11**(1).
35. Wang T, Wang D, Zhang L, Yang P, Wang J, Liu Q, Yan F, Lin F: **The TGFbeta-miR-499a-SHKBP1 pathway induces resistance to EGFR inhibitors in osteosarcoma cancer stem cell-like cells.** *J Exp Clin Cancer Res* 2019, **38**(1):226.
- 25 36. Izumchenko E, Chang X, Michailidi C, Kagohara L, Ravi R, Paz K, Brait M, Hoque MO, Ling S, Bedi A *et al*: **The TGFbeta-miR200-MIG6 pathway orchestrates the EMT-associated kinase switch that induces resistance to EGFR inhibitors.** *Cancer Res* 2014, **74**(14):3995-4005.
- 30 37. Park KS, Raffeld M, Moon YW, Xi L, Bianco C, Pham T, Lee LC, Mitsudomi T, Yatabe Y, Okamoto I *et al*: **CRIPTO1 expression in EGFR-mutant NSCLC elicits intrinsic EGFR-inhibitor resistance.** *J Clin Invest* 2014, **124**(7):3003-3015.
38. Lee CC, Ho HC, Su YC, Lee MS, Hung SK, Lin CH: **MCP1-Induced Epithelial-Mesenchymal Transition in Head and Neck Cancer by AKT Activation.** *Anticancer Res*  
35 2015, **35**(6):3299-3306.
39. Chen X, Zhu M, Zou X, Mao Y, Niu J, Jiang J, Dong T, Shi Y, Yang X, Liu P: **CCL2-targeted ginkgolic acid exerts anti-glioblastoma effects by inhibiting the JAK3-STAT1/PI3K-AKT signaling pathway.** *Life Sci* 2022, **311**(Pt B):121174.

40. Jin J, Lin J, Xu A, Lou J, Qian C, Li X, Wang Y, Yu W, Tao H: **CCL2: An Important Mediator Between Tumor Cells and Host Cells in Tumor Microenvironment.** *Front Oncol* 2021, **11**:722916.
41. Xu J, Lin H, Li G, Sun Y, Shi L, Ma WL, Chen J, Cai X, Chang C: **Sorafenib with ASC-J9(®) synergistically suppresses the HCC progression via altering the pSTAT3-CCL2/Bcl2 signals.** *Int J Cancer* 2017, **140**(3):705-717.
- 5
42. Zhou SL, Zhou ZJ, Hu ZQ, Huang XW, Wang Z, Chen EB, Fan J, Cao Y, Dai Z, Zhou J: **Tumor-Associated Neutrophils Recruit Macrophages and T-Regulatory Cells to Promote Progression of Hepatocellular Carcinoma and Resistance to Sorafenib.** *Gastroenterology* 2016, **150**(7):1646-1658.e1617.
- 10
43. Feng H, Liu K, Shen X, Liang J, Wang C, Qiu W, Cheng X, Zhao R: **Targeting tumor cell-derived CCL2 as a strategy to overcome Bevacizumab resistance in ETV5(+) colorectal cancer.** *Cell Death Dis* 2020, **11**(10):916.
44. Shi P, Oh YT, Deng L, Zhang G, Qian G, Zhang S, Ren H, Wu G, Legendre B, Jr., Anderson E *et al*: **Overcoming Acquired Resistance to AZD9291, A Third-Generation EGFR Inhibitor, through Modulation of MEK/ERK-Dependent Bim and Mcl-1 Degradation.** *Clin Cancer Res* 2017, **23**(21):6567-6579.
- 15
45. Huang WC, Yadav VK, Cheng WH, Wang CH, Hsieh MS, Huang TY, Lin SF, Yeh CT, Kuo KT: **The MEK/ERK/miR-21 Signaling Is Critical in Osimertinib Resistance in EGFR-Mutant Non-Small Cell Lung Cancer Cells.** *Cancers (Basel)* 2021, **13**(23).
- 20
46. Chaib I, Karachaliou N, Pilotto S, Codony Servat J, Cai X, Li X, Drozdowskyj A, Servat CC, Yang J, Hu C *et al*: **Co-activation of STAT3 and YES-Associated Protein 1 (YAP1) Pathway in EGFR-Mutant NSCLC.** *J Natl Cancer Inst* 2017, **109**(9).
47. Kim SM, Kwon OJ, Hong YK, Kim JH, Solca F, Ha SJ, Soo RA, Christensen JG, Lee JH, Cho BC: **Activation of IL-6R/JAK1/STAT3 signaling induces de novo resistance to irreversible EGFR inhibitors in non-small cell lung cancer with T790M resistance mutation.** *Mol Cancer Ther* 2012, **11**(10):2254-2264.
- 25
48. Lee HJ, Zhuang G, Cao Y, Du P, Kim HJ, Settleman J: **Drug resistance via feedback activation of Stat3 in oncogene-addicted cancer cells.** *Cancer Cell* 2014, **26**(2):207-221.
- 30
49. Zhao C, Li H, Lin HJ, Yang S, Lin J, Liang G: **Feedback Activation of STAT3 as a Cancer Drug-Resistance Mechanism.** *Trends Pharmacol Sci* 2016, **37**(1):47-61.
50. Sun Y, Dong Y, Liu X, Zhang Y, Bai H, Duan J, Tian Z, Yan X, Wang J, Wang Z: **Blockade of STAT3/IL-4 overcomes EGFR T790M-cis-L792F-induced resistance to osimertinib via suppressing M2 macrophages polarization.** *EBioMedicine* 2022, **83**:104200.
- 35
51. Yoshida T, Song L, Bai Y, Kinose F, Li J, Ohaegbulam KC, Munoz-Antonia T, Qu X, Eschrich S, Uramoto H *et al*: **ZEB1 Mediates Acquired Resistance to the Epidermal Growth Factor Receptor-Tyrosine Kinase Inhibitors in Non-Small Cell Lung Cancer.**

*PLoS One* 2016, **11**(1):e0147344.

52. Zhang T, Guo L, Creighton CJ, Lu Q, Gibbons DL, Yi ES, Deng B, Molina JR, Sun Z, Yang P *et al*: **A genetic cell context-dependent role for ZEB1 in lung cancer.** *Nat Commun* 2016, **7**:12231.
- 5 53. Wang YY, Vadhan A, Chen PH, Lee YL, Chao CY, Cheng KH, Chang YC, Hu SC, Yuan SF: **CD44 Promotes Lung Cancer Cell Metastasis through ERK-ZEB1 Signaling.** *Cancers (Basel)* 2021, **13**(16).

## Figure Captions

### Fig. 1. CCL2 is elevated in EGFR TKI-resistant cell lines.

(A, E) Viability of human lung cancer cell cells treated with osimertinib determined using MTT assay. (B, F) Expression of mRNA of CCL2 in the indicated cell lines was evaluated using RT-pPCR. The mRNA bar graph represents the mean±SD of three independent experiments (\*\*p < 0.001; Student's t-test). (D, H) Expression level of CCL2 protein in the indicated cell lines was evaluated using western blot analysis. (C, G) ELISA was used to determine the CCL2 levels in the conditional medium of H1975, H1975/AZD-15, H1975/AZD-18, HCC827, and HCC827/gef cells. (\*\*p < 0.001; Student's t-test) (I) CCL2 mRNA expression levels were detected using RT-qPCR from the primary cancer cells collected from 63 malignant pleural effusions of patients with lung adenocarcinoma. Treatment-naïve patients with lung cancer (n = 26); lung cancer patients with acquired resistance to osimertinib (n = 16); lung cancer patients with acquired resistance to other first- or second-generation EGFR-TKIs (gefitinib, erlotinib or afatinib; n = 21). The statistical comparison between the two groups was performed using the Mann–Whitney U test.

15

### Fig. 2. CCL2 increased the resistance of lung cancer cells to osimertinib

(A) The expression level of CCL2 was detected using RT-qPCR (right) and western blot (left) in CCL2-overexpressing and the corresponding control cells (\*\*p < 0.001). (B) HCC872-CCL2 cells were treated with indicated concentrations for 48 h; cell viability was determined using MTT assays. The viability of



DMSO-treated control cells was set to 100%. Error bars showed the SD for  $n = 4$  independent experiments (\*\*\*)  $p < 0.001$ ). (C) Caspase-9 activity was measured using luminescent Caspase-Glo 9 assay. (\*\*\*)  $p < 0.001$ ). (D) The xenograft growth curve between HCC827-mock and HCC827-CCL2 mice groups showed an elevation of tumor size. Tumor volume was measured every 4 days. Each data point was the mean tumor volume ( $\text{mm}^3$ ), and error bars indicate the standard error (ns, not statistically significant). (E) Mice were treated with 0.5 mg/kg osimertinib daily via oral gavage for 32 days ( $n = 5$  in each subgroup). (\* $p < 0.05$ ) (F) Tumor weight of the tumors dissected from the HCC872-CCL2 bearing xenograft mouse model. The p-value was determined using the Student's t-test (\* $p < 0.05$ ).

### 10 **Fig. 3. Silencing CCL2 expression re-sensitizes cancer cells to osimertinib treatment**

(A, F, and I) The CCL2 expression level was measured using RT-qPCR (right) and western blot (left) in CCL2-knockdown and the corresponding control transfectants (\*\*\*)  $p < 0.001$ ). (B, G, and J) The cellular viability of CCL2-knockdown and control transfectants was determined following treatment with various doses of osimertinib for 72 h using MTT assay (\*\*\*)  $p < 0.001$ ). (C) The CCL2-knockdown (HCC827/gef-si-CCL2-1 and HCC827/gef-si-CCL2-2) and control transfectants were exposed to 500 nM of osimertinib for 24 h. Caspase-9 activity was measured using luminescent Caspase-Glo 9 assay. Error bars represent the SD for  $n = 3$  independent experiments (\*\*\*)  $p < 0.001$  and (\*\*\*)  $p < 0.01$ ). (D) The cells were double stained with annexin V–fluorescein isothiocyanate and propidium iodide and analyzed using flow cytometry. The annexin-V-positive cells represented apoptotic cells. The bar chart displays the

distribution of apoptotic cells as a percentage and is derived from three independent experiments (\*\*p < 0.01 compared to vehicle control). (E, H, and K) Cleaved poly-ADP-ribose polymerase (PARP) and caspase-3 of the CCL2-knockdown and control cells were assayed using western blot.

5 **Fig. 4. Zeb1 is required to CCL2-induced acquired resistance to osimertinib**

(A) The morphology of indicated cell lines is shown in the image obtained via microscopy (left).

Differential expression of the epithelial marker (E-cadherin; E-cad), mesenchymal markers (vimentin; VIM), and EMT regulators (Zeb1, Snail, and Slug) was examined using western blot (right). (B) The

morphology of HCC827 and HCC827/gef cells was shown in the image obtained via microscopy (left).

10 The expression of E-cad, VIM, Zeb1, Snail, and Slug was examined using western blot analysis. The loading control was  $\alpha$ -tubulin (right). (C, D) The expression of EMT regulators (Zeb1, Snail, and Slug)

in HCC827-CCL2 and CCL2 knockdown transfectants (HCC827/gef-si-CCL2-1, H1975/AZD-18-si-CCL2-1) was detected using western blot. HCC827-mock, HCC827/gef-si-scramble, and H1975/AZD-

18-si-scramble were the control groups. (E, G) HCC827-CCL2 and H1975/AZD-18 cells were knocked

15 down with Zeb1 siRNA, and the expression of Zeb1 mRNA and protein was detected using RT-qPCR and western blot (\*\*p<0.001). (F, H) The cellular viability of Zeb1-knockdown (HCC827CCL2-si-Zeb1

and H1975/AZD-18-si-Zeb1) and control transfectants was determined following treatment with various doses of osimertinib for 48 h in MTT assays. (n = 4 independent experiments, \*\*p<0.001).

**Fig. 5. CCL2 activates STAT3 and ERK signaling pathways**

(A, B) Expression levels of EGFR and other EGFR downstream molecules of osimertinib-sensitive cells and resistant cells were detected in the absence or presence of 250 nM osimertinib for 3 h. (C) The expressions of p-AKT, p-ERK1/2, and p-STAT3 in H1975 and HCC827 cells were detected after the treatment of 20 ng/mL recombinant human CCL2 proteins (rCCL2) for 4 h, followed by western blot analysis. (D, E) Expressions of p-AKT, p-ERK1/2, and p-STAT3 in CCL2-overexpressing and CCL2-knockdown transfectants were analyzed, with  $\alpha$ -tubulin serving as the loading control.

**Fig. 6. CCL2 contributes to osimertinib resistance via participation of the STAT3 and ERK signaling pathways**

(A) The CCR2 expression level was measured using RT-qPCR (left) (\*\*p < 0.01) and western blot (right) in HCC827-CCL2 cells with CCR2 siRNA. (B) HCC827-CCL2-si-CCR2 cells were treated with osimertinib as indicated for 48 h; cell viability was determined using MTT assays. The viability of vehicle control cells was set to 100% (\*\*p < 0.001). (C) Caspase-9 activity was measured using luminescent Caspase-Glo 9 assay. (\*\*p < 0.001 compared to HCC827-CCL2-si-scramble). (D) After treatment of INCB3344 in HCC827-CCL2 cells, the expression of CCR2 downstream kinases, including p-STAT3, p-ERK1/2, STAT3, ERK1/2, and Zeb1, was measured using western blot. (E) The HCC827-CCL2 cells were seeded into 96-well plates, followed by a 48-h treatment with the vehicle, INCB3344 alone, osimertinib alone, or a combination of both drugs (\*p < 0.05). (F) Caspase-9 activity was measured using

luminescent Caspase-Glo 9 assay (\*\* $p < 0.01$ ). (G) HCC827-CCL2 cells were treated with the vehicle (DMSO) or 40  $\mu$ M S3I-201 for 24 h and subsequently harvested for western blot analysis against p-STAT3, p-ERK1/2, STAT3, ERK1/2, and Zeb1. (H) Following osimertinib and S3I-201 treatment alone or in combination for 48 h, the viability of HCC827-CCL2 cells was determined by MTT. (\*\* $p < 0.01$ ) (I) Tumor volume of H1975/AZD-18 xenografts treated with vehicle, osimertinib (1 mg/kg/day), S3I-201 (5 mg/kg/2day), or a combination of both drugs for 16 days ( $n = 5$  in each subgroup). Error bars indicate the standard error (\* $p < 0.05$ ). (J) The expression of p-STAT3, p-ERK1/2, STAT3, ERK, and Zeb1 in HCC827-CCL2 cells with ERK inhibitor selumetinib was measured using western blot analysis. (K) HCC827-CCL2 cells were treated with osimertinib and selumetinib treatment alone or in combination for 48 h; cell viability was determined using MTT assays (\*\* $p < 0.001$ ).

**Fig. 7. Model of the regulatory signaling networks of CCL2-CCR2-STAT3/ERK-Zeb1 in osimertinib resistance.**

**Fig S1. STAT3 and ERK pathways mediate the CCL2-induced EMT phenotype.** (A) HCC827-CCL2 cells were transfected with 75 nM CCR2 siRNA for 48 h. Whole-cell protein extracts were subjected to western blot analysis using E-cadherin and vimentin antibodies, with  $\alpha$ -tubulin as an internal loading control. HCC827-CCL2 cells treated with INCB3344 (B), S3I-201 (C), and selumetinib (D) were harvested, and E-cadherin and vimentin protein levels were assessed using western blot.

Fig 1 (Chang TH)

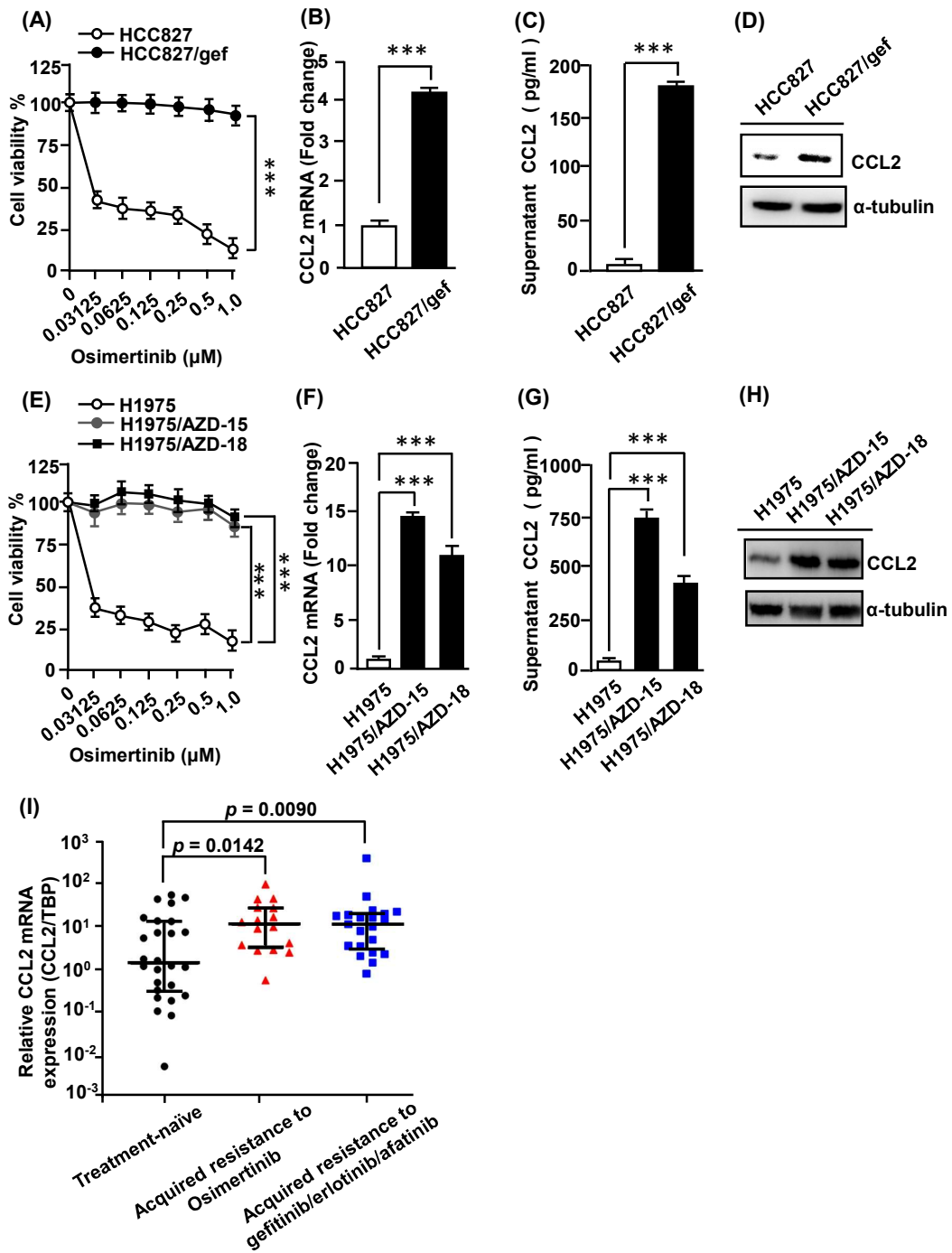


Fig 2 (Chang TH)

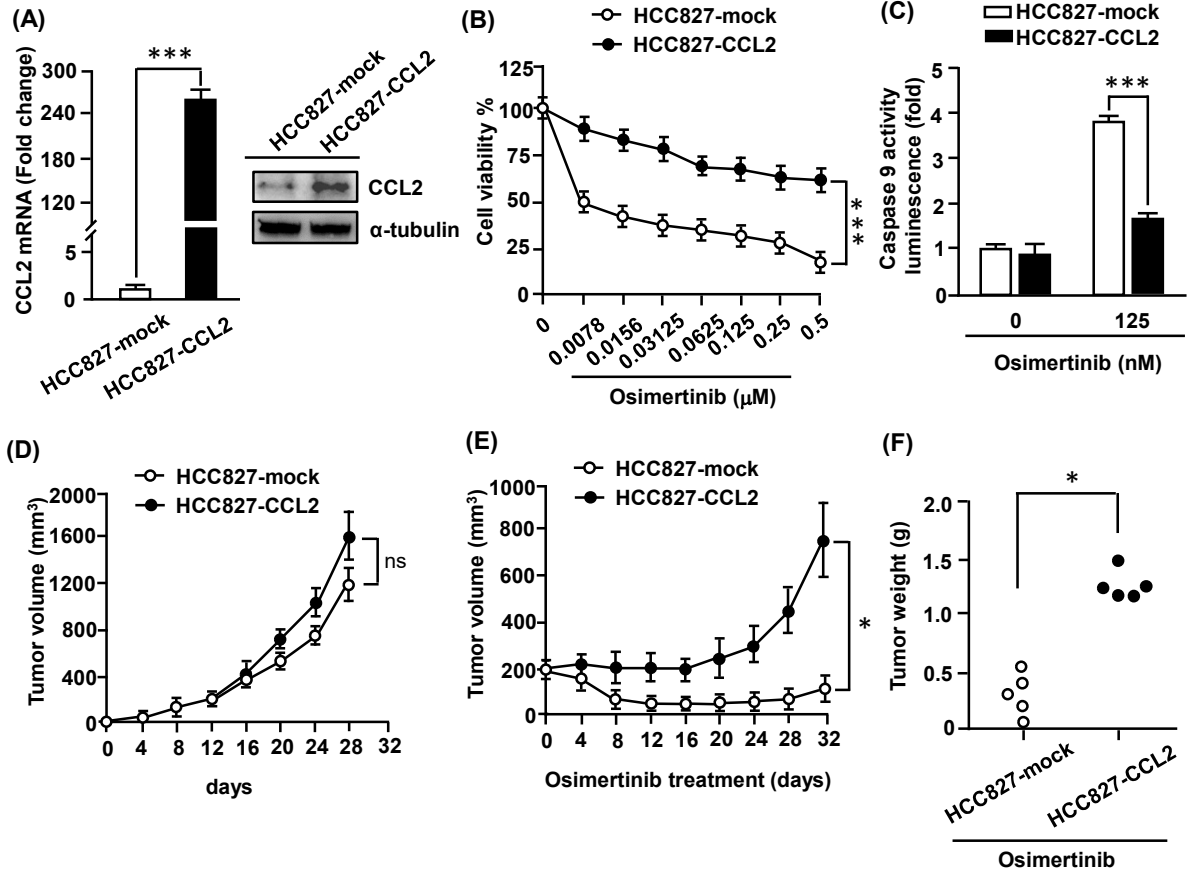


Fig 3 (Chang TH)

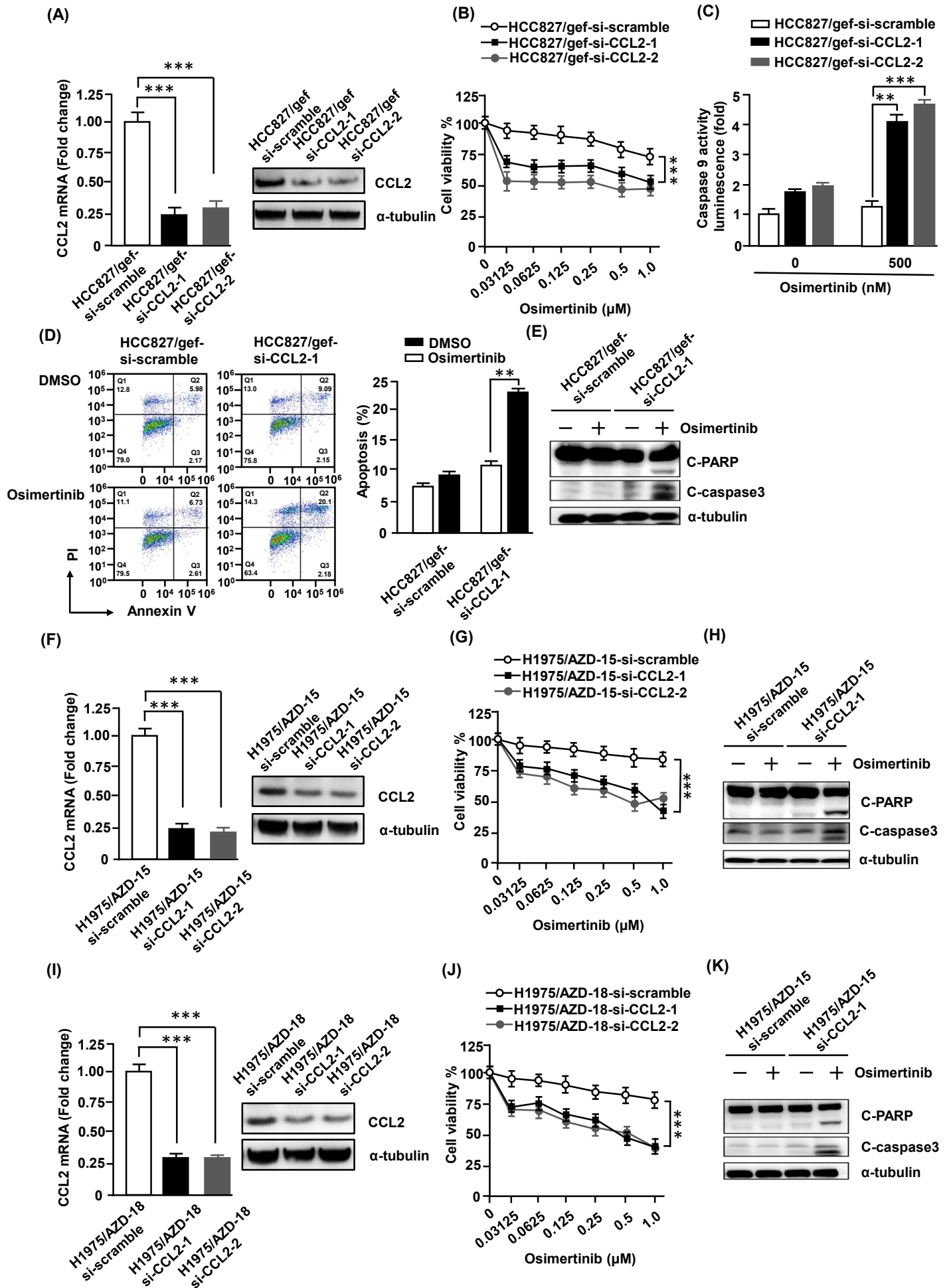


Fig 4 (Chang TH)

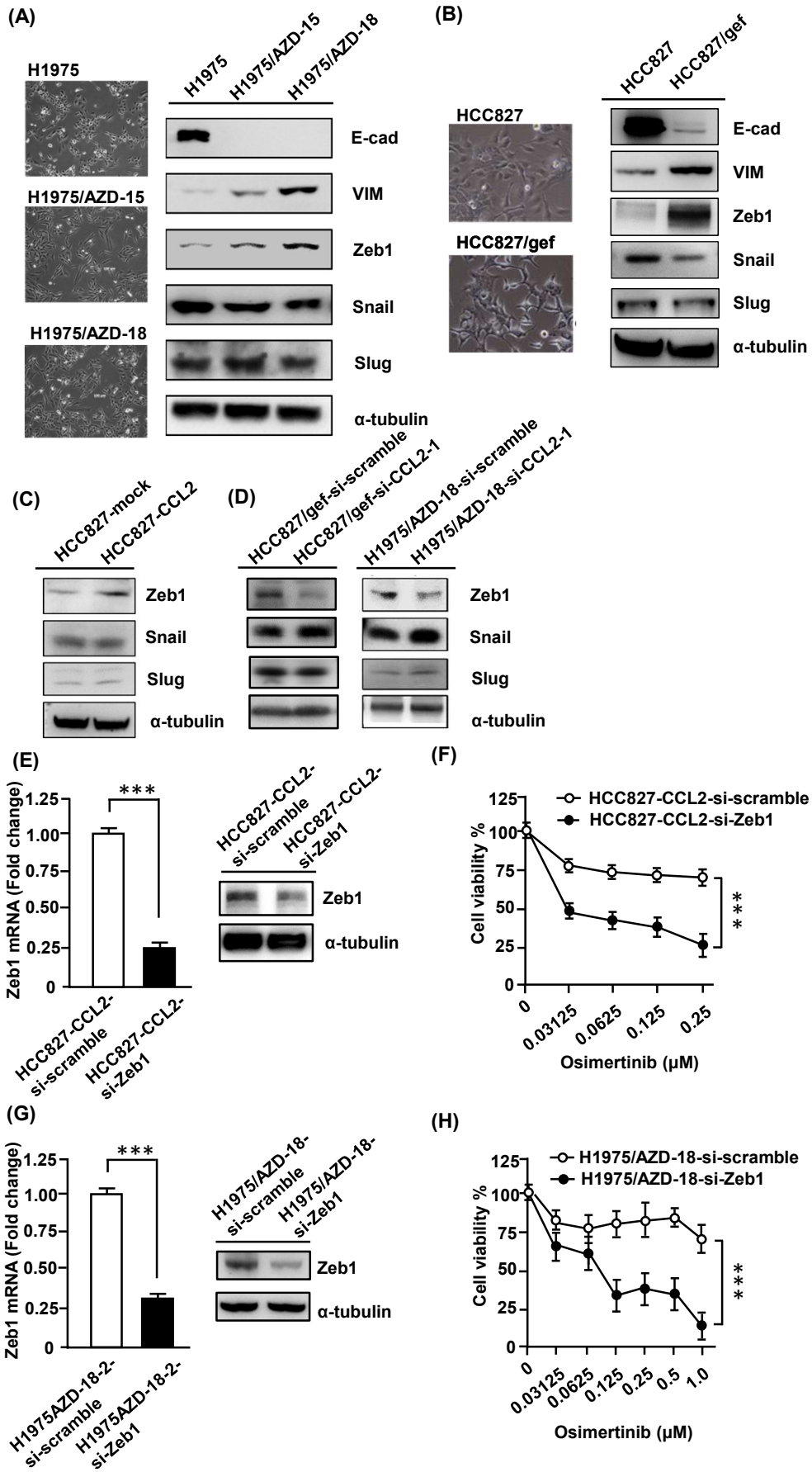




Fig 5 (Chang TH)

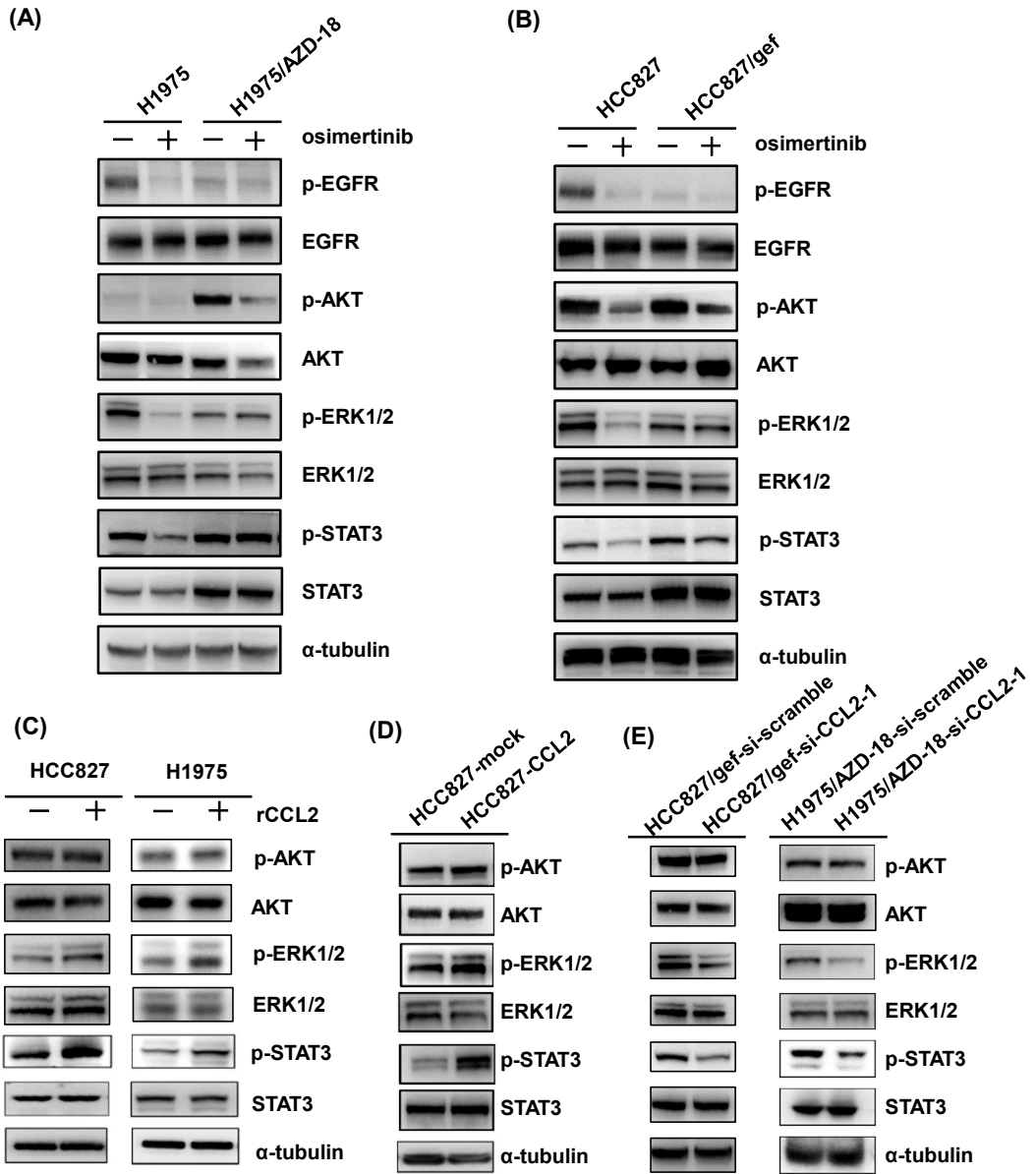


Fig 6 (Chang TH)

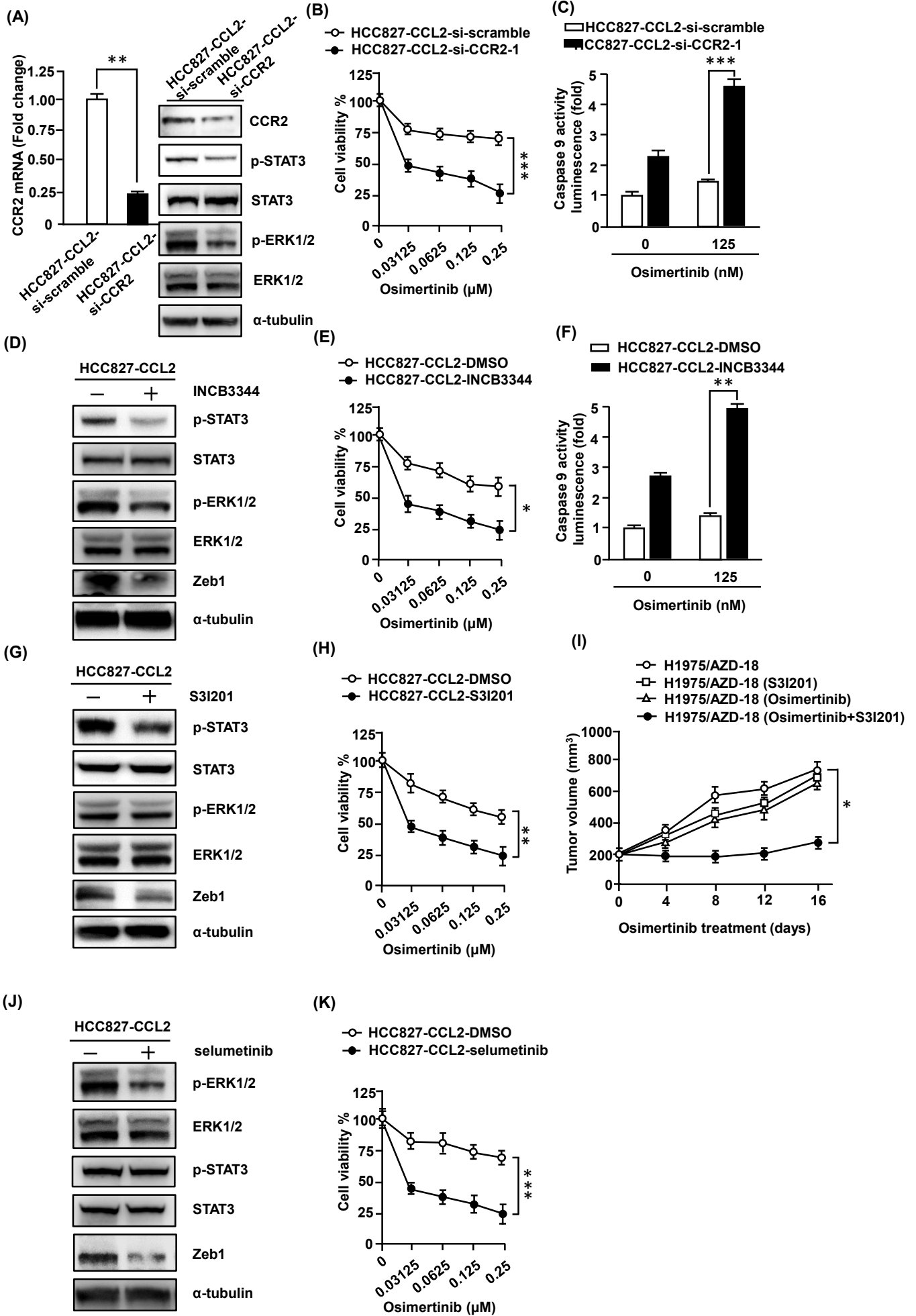
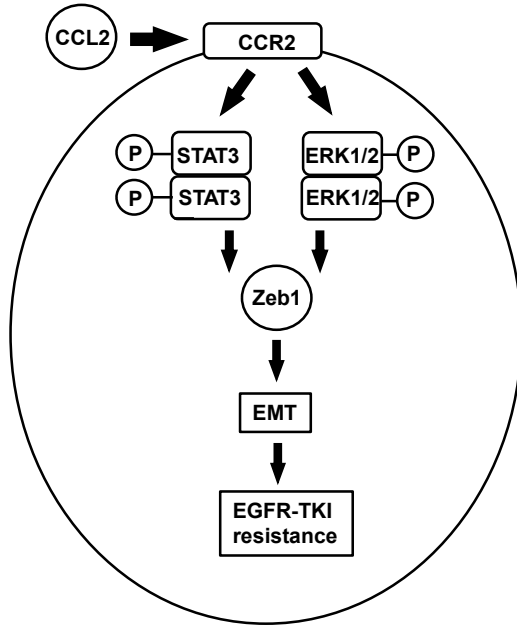
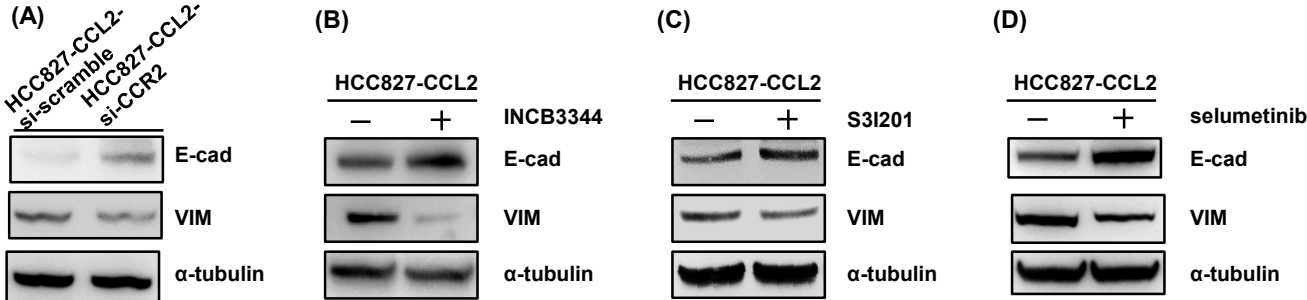


Fig 7 (Chang TH)



Supplementary Fig 1 (Chang TH)



## Supplementary Tables

**Table S1. Antibodies used for western blot in the study**

Name	Catalog	Company	Host	Application
CCL2	GTX60582	GeneTex	mouse	WB
Zeb1	GTX105278	GeneTex	rabbit	WB
Snail	GTX125918	GeneTex	rabbit	WB
p-EGFR (Tyr1068)	#2236	Cell signaling	mouse	WB
EGFR	SC-03	Santa cruz	rabbit	WB
p-AKT(Ser473)	#4060	Cell signaling	rabbit	WB
AKT	#9272	Cell signaling	rabbit	WB
p-ERK1/2 (Thr202/Tyr204)	#9101	Cell signaling	rabbit	WB
ERK1/2	#9102	Cell signaling	rabbit	WB
p-STAT3 (Tyr705)	GTX61820	GeneTex	rabbit	WB
STAT3	#4904	Cell signaling	rabbit	WB
CCR2	#12199	Cell signaling	rabbit	WB
Slug	ab27568	Abcam	rabbit	WB
PARP	#9542	Cell signaling	rabbit	WB
Cleaved Caspase-3	#9664	Cell signaling	rabbit	WB
E-cadherin	610181	BD	mouse	WB
vimentin	5741S	Cell Signaling	rabbit	WB
$\alpha$ -tubulin	#05-829	Millipore	mouse	WB

**Table S2. Primers used for quantitative real-time PCR**

Gene names	Forward	Reverse
TBP	5'-ACGCCAGCTTCGGAGAGTT-3'	5'-CCTCATGATTACCGCAGCAAA-3'
CCL2	5'-AAGATCTCAGTGCAGAGGCTCG-3'	5'-TTGCTTGTCCAGGTGGTCCAT-3'
Zeb1	5'-TGACAGAAAGGAAGGGCAAGA-3'	5'-CAGGTGAGTAATTGTGAAAATGCATGT-3'
CCR2	5'-CACAAGCTGAACAGAGAAAGTGGAT-3'	5'-GAACGAGATGTGGACAGCATGT-3'

**Table S3. Top 100 EGFR TKI resistance-related genes.**

Rank	gene_id	gene_name	gene_type	score
1	ENSG00000163453	IGFBP7	protein_coding	3.85
2	ENSG00000129965	INS-IGF2	protein_coding	3.64
3	ENSG00000148677	ANKRD1	protein_coding	3.48
4	ENSG00000143546	S100A8	protein_coding	3.45
5	ENSG00000118523	CTGF	protein_coding	3.42
6	ENSG00000207279	SNORD116-24	snoRNA	3.37
7	ENSG00000164379	FOXQ1	protein_coding	3.23
8	ENSG00000151892	GFRA1	protein_coding	3.18
9	ENSG00000115461	IGFBP5	protein_coding	3.10
10	ENSG00000119714	GPR68	protein_coding	2.69
11	ENSG00000165092	ALDH1A1	protein_coding	2.65
12	ENSG00000145934	TENM2	protein_coding	2.57
13	ENSG00000155622	XAGE2	protein_coding	2.55
14	ENSG00000138131	LOXL4	protein_coding	2.40
15	ENSG00000168386	FILIP1L	protein_coding	2.40
16	ENSG00000130176	CNN1	protein_coding	2.36
17	ENSG00000108691	CCL2	protein_coding	2.30
18	ENSG00000230043	TMSB4XP6	processed_pseudogene	2.24
19	ENSG00000175984	DENND2C	protein_coding	2.16
20	ENSG00000153707	PTPRD	protein_coding	2.13
21	ENSG00000078401	EDN1	protein_coding	2.10
22	ENSG00000115008	IL1A	protein_coding	2.08
23	ENSG00000123610	TNFAIP6	protein_coding	2.07
24	ENSG00000244067	GSTA2	protein_coding	2.02
25	ENSG00000175928	LRRN1	protein_coding	2.01
26	ENSG00000213626	LBH	protein_coding	1.98
27	ENSG00000106366	SERPINE1	protein_coding	1.97
28	ENSG00000125538	IL1B	protein_coding	1.94
29	ENSG00000260604	AL590004.4	lincRNA	1.93
30	ENSG00000077782	FGFR1	protein_coding	1.93
31	ENSG00000076716	GPC4	protein_coding	1.91
32	ENSG00000144476	ACKR3	protein_coding	1.90
33	ENSG00000125740	FOSB	protein_coding	1.89
34	ENSG00000073756	PTGS2	protein_coding	1.88
35	ENSG00000207174	SNORD116-15	snoRNA	1.85
36	ENSG00000101335	MYL9	protein_coding	1.85

37	ENSG00000184500	PROS1	protein_coding	1.84
38	ENSG00000206621	SNORD116-14	snoRNA	1.83
39	ENSG00000173706	HEG1	protein_coding	1.82
40	ENSG00000118785	SPP1	protein_coding	1.82
41	ENSG00000134258	VTCN1	protein_coding	1.81
42	ENSG00000117114	ADGRL2	protein_coding	1.79
43	ENSG00000112299	VNN1	protein_coding	1.76
44	ENSG00000117020	AKT3	protein_coding	1.76
45	ENSG00000128422	KRT17	protein_coding	1.73
46	ENSG00000173391	OLR1	protein_coding	1.73
47	ENSG00000091986	CCDC80	protein_coding	1.72
48	ENSG00000153071	DAB2	protein_coding	1.72
49	ENSG00000108342	CSF3	protein_coding	1.71
50	ENSG00000115009	CCL20	protein_coding	1.70
51	ENSG00000164125	FAM198B	protein_coding	1.69
52	ENSG00000163734	CXCL3	protein_coding	1.69
53	ENSG00000261040	WFDC21P	processed_transcript	1.69
54	ENSG00000207014	SNORD116-3	snoRNA	1.68
55	ENSG00000165685	TMEM52B	protein_coding	1.68
56	ENSG00000124102	PI3	protein_coding	1.67
57	ENSG00000180537	RNF182	protein_coding	1.67
58	ENSG00000163283	ALPP	protein_coding	1.66
59	ENSG00000122641	INHBA	protein_coding	1.65
60	ENSG00000210077	MT-TV	Mt_tRNA	1.64
61	ENSG00000170390	DCLK2	protein_coding	1.64
62	ENSG00000186340	THBS2	protein_coding	1.63
63	ENSG00000207093	SNORD116-8	snoRNA	1.61
64	ENSG00000137801	THBS1	protein_coding	1.61
65	ENSG00000183688	RFLNB	protein_coding	1.59
66	ENSG00000182326	C1S	protein_coding	1.59
67	ENSG00000169429	CXCL8	protein_coding	1.55
68	ENSG00000166250	CLMP	protein_coding	1.54
69	ENSG00000109511	ANXA10	protein_coding	1.54
70	ENSG00000081052	COL4A4	protein_coding	1.53
71	ENSG00000176907	C8orf4	protein_coding	1.52
72	ENSG00000144810	COL8A1	protein_coding	1.52
73	ENSG00000236091	LINC02243	lincRNA	1.51
74	ENSG00000243955	GSTA1	protein_coding	1.50



75	ENSG00000137393	RNF144B	protein_coding	1.50
76	ENSG00000172575	RASGRP1	protein_coding	1.49
77	ENSG00000158186	MRAS	protein_coding	1.48
78	ENSG00000207001	SNORD116-2	snoRNA	1.48
79	ENSG00000120129	DUSP1	protein_coding	1.48
80	ENSG00000170558	CDH2	protein_coding	1.48
81	ENSG00000207442	SNORD116-6	snoRNA	1.48
82	ENSG00000231389	HLA-DPA1	protein_coding	1.48
83	ENSG00000142871	CYR61	protein_coding	1.48
84	ENSG00000131459	GFPT2	protein_coding	1.48
85	ENSG00000134668	SPOCD1	protein_coding	1.47
86	ENSG00000167601	AXL	protein_coding	1.46
87	ENSG00000085563	ABCB1	protein_coding	1.46
88	ENSG00000165376	CLDN2	protein_coding	1.46
89	ENSG00000176046	NUPR1	protein_coding	1.46
90	ENSG00000166741	NNMT	protein_coding	1.45
91	ENSG00000131378	RFTN1	protein_coding	1.45
92	ENSG00000111305	GSG1	protein_coding	1.45
93	ENSG00000131016	AKAP12	protein_coding	1.44
94	ENSG00000086289	EPDR1	protein_coding	1.44
95	ENSG00000139278	GLIPR1	protein_coding	1.44
96	ENSG00000130433	CACNG6	protein_coding	1.43
97	ENSG00000166033	HTRA1	protein_coding	1.43
98	ENSG00000171711	DEFB4A	protein_coding	1.42
99	ENSG00000185275	CD24P4	processed_pseudogene	1.42
100	ENSG00000100100	PIK3IP1	protein_coding	1.42

**Table S4.** The pleural effusion from the 63 patients with advanced lung adenocarcinoma who received EGFR-TKI therapies

	<b>Treatment-naive</b>	<b>Acquired resistance to osimertinib</b>	<b>Acquired resistance to 1<sup>st</sup>/2<sup>nd</sup>-G TKIs*</b>	<b><i>p</i>-value</b>
<b>Total No.</b>	26	16	21	
<b>Age, median years (range)</b>	66.4 (43.5–85.2)	73.9 (40.1–90.0)	63.6 (29.7–91.4)	0.063 <sup>#</sup>
<b>Sex</b>				0.906
<b>Female</b>	17	11	15	
<b>Male</b>	9	5	6	
<b>Smoking</b>				0.665
<b>Nonsmokers</b>	22	15	18	
<b>Smokers</b>	4	1	3	
<b>EGFR mutation</b>				0.478
<b>Del-19</b>	14	11	14	
<b>L858R</b>	11	5	5	
<b>Other</b>	1	0	2	

<sup>#</sup> By Kruskal–Wallis test; \* 1<sup>st</sup>/2<sup>nd</sup>-G TKIs: 1<sup>st</sup>- or 2<sup>nd</sup>-generation EGFR TKIs

Del-19: Deletion in exon 19; EGFR TKI: Epidermal growth factor receptor tyrosine kinase inhibitor